
Supporting Information

Synthesis of trityl radical-conjugated disulfide biradicals for the measurement of thiol concentration

Yangping Liu,[†] Yuguang Song,[†] Antal Rockenbauer,[§] Jian Sun,[†] Craig Hemann,[†]
Frederick A. Villamena,^{†,‡} and Jay L. Zweier^{†,*}

[†]Center for Biomedical EPR Spectroscopy and Imaging, The Davis Heart and Lung Research Institute, the Division of Cardiovascular Medicine, Department of Internal Medicine and [‡]Department of Pharmacology, College of Medicine, The Ohio State University, Columbus, OH, 43210, USA, [§]Chemical Research Center, Institute of Structural Chemistry, P.O. Box 17, H-1525 Budapest, Hungary.

Email: jay.zweier@osumc.edu

Supplementary Materials Table of Contents

I. The purity analysis of TSSN and TSST using TEMPOL	S2-3
II. HPLC analysis of TSSN and TSST	S3-4
III. Concentration effect on the EPR spectra of TSSN and TSST	S4-5
IV. Temperature effect on the spectra of TSST	S5
V. EPR simulation	S6-7
VI. Reaction of TSSN with GSH detected by UV-Vis spectroscopy	S7
VII. Kinetic studies of TSSN and TSST with GSH detected by EPR spectroscopy	S8-9
VIII. Reaction of TSSN with ascorbate	S10-11
IX. Plot of UV-vis absorbance versus GSH concentration	S11
X. Spectroscopic characterization	S12-14

I. The purity analysis of TSSN and TSST using TEMPOL

The biradical purity was determined using 4-hydroxy-2,2,6,6-tetramethylpiperidine-N-oxyl (TEMPOL) as standard. In a typical experiment, the purified biradical as a carboxylate form was weighed and dissolved in phosphate buffer (PB, 50 mM, pH 7.4). The EPR spectrum was obtained and peak area was determined using double integration. The concentration of the biradical was then determined using a standard curve of known concentration of TEMPOL versus peak area (Figure S1 and S2). Each experiment was done in triplicate. The paramagnetic purity for TSSN and TSST was determined to $96.3 \pm 1.2\%$ and $94.7 \pm 1.8\%$, respectively.

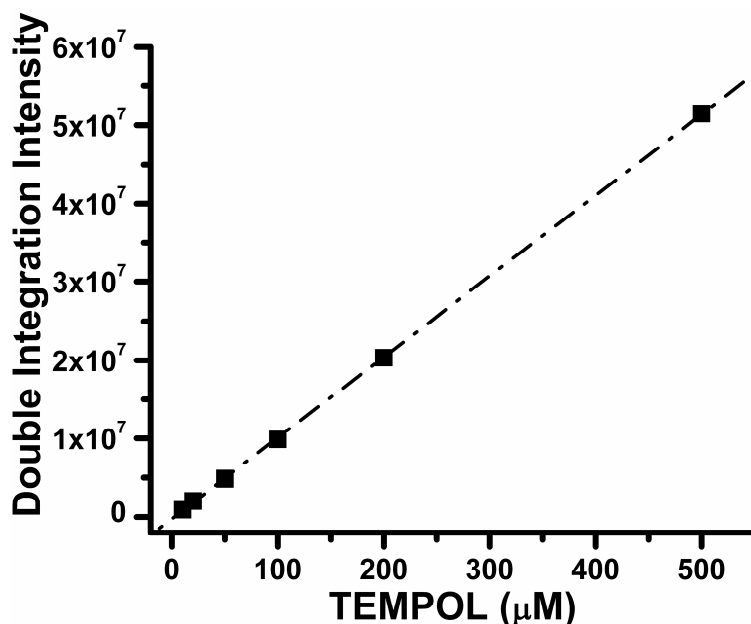


Figure S1. The EPR signal integration of TEMPOL as a function of the concentration in water. EPR spectra were recorded with 10 mW microwave power, 1 G modulation amplitude. The TSSN concentration was determined using this curve.

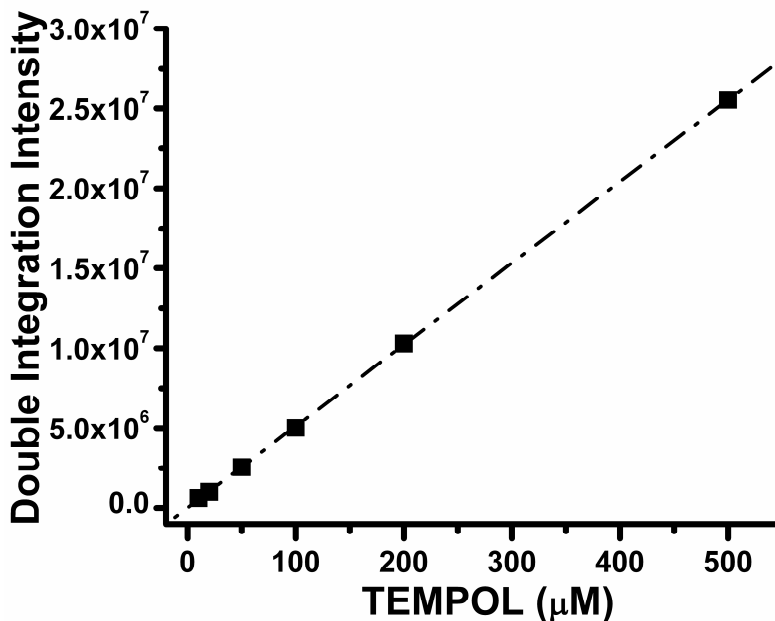


Figure S2. The EPR signal integration of TEMPOL as a function of the concentration in water. EPR spectra were recorded with 2 mW microwave power, 0.2 G modulation amplitude. The TSST concentration was determined using this curve.

II. HPLC analysis of TSSN and TSST

Briefly, 20 μl of 200 μM TSSN and TSST were injected separately into the HPLC system (CoulArray System from ESA Analytical, Ltd. Chelmsford, MA) on a Supelcosil LC-18-T column (4.6 x 150 mm, 3 micron, Sigma) with automated gradient controller, refrigerated autosampler, and ESA software for data collection and analysis. The mobile phase consists of the medium A containing 20 mM ammonium acetate (pH 7.0) and medium B containing 20 mM ammonium acetate: methanol : acetonitrile = 40 : 20 : 40 (v : v : v) (pH 7.0) at a flow rate of 1.0 ml/min. Gradient applied was: 0 ~ 3min, 40% B; 3 ~ 18 min, 80% B; 18 ~ 28min, 85% B; 28 ~ 30min, 40% B; followed by 15 min equilibration of 40% B before next injection. The compounds were detected at 469 nm by

the UV-Vis detector serially connected to the column. Under experimental conditions, only one peak was observed for each compound. The retention time is 22.6 min for TSSN and 27.5 min for TSST.

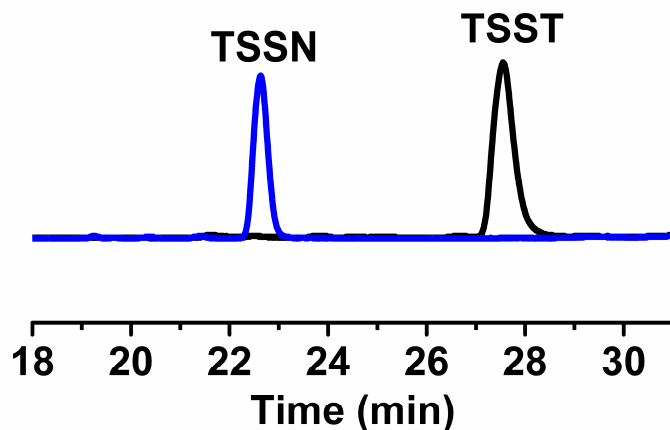


Figure S3. HPLC chromatograms of TSSN and TSST.

III. Concentration effect on the EPR spectra of TSSN and TSST

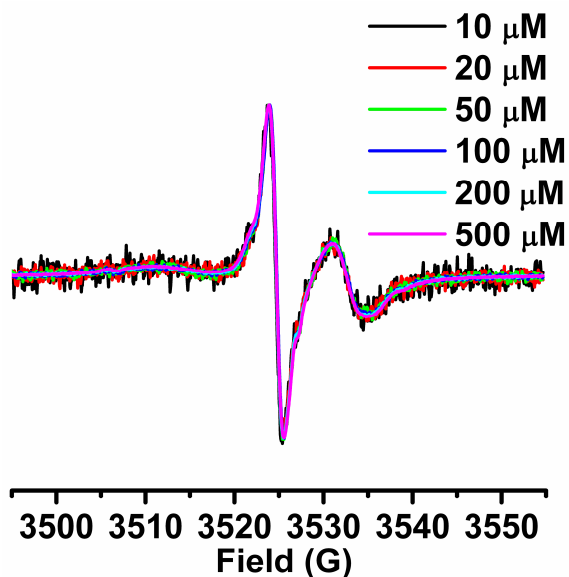


Figure S4. EPR spectra of TSSN at different concentrations in PB (pH 7.4, 20 mM) at room temperature. The spectra were scaled to the same maximum lineheight.

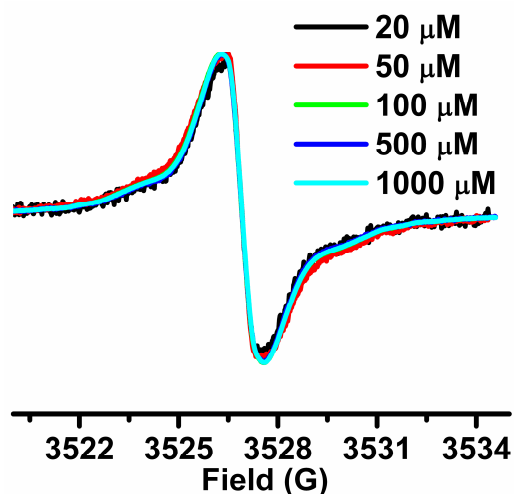


Figure S5. EPR spectra of TSST at different concentrations in PB (pH 7.4, 20 mM) at room temperature. The spectra were scaled to the same maximum lineheight.

IV. Temperature effect on the spectra of TSST

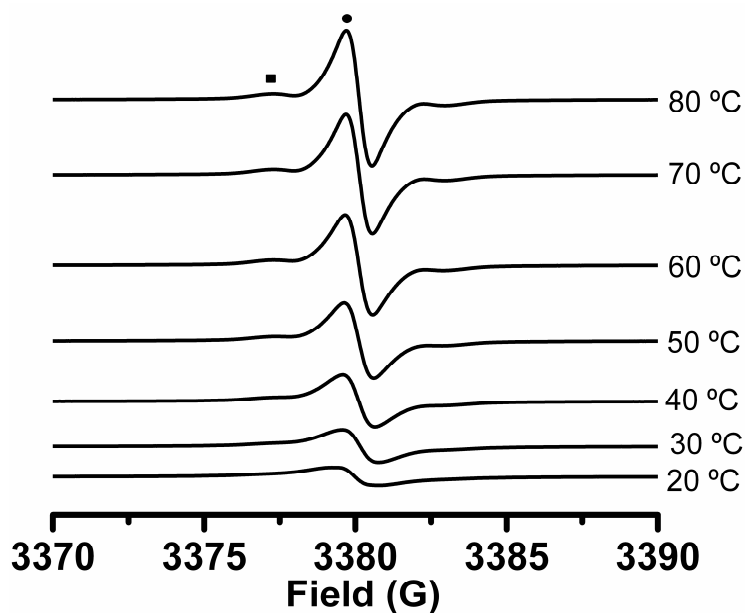


Figure S6. EPR spectra of TSST at different temperatures in PB (pH 7.4, 20 mM). (●) the singlet signal; (■) the doublet signal.

V. EPR simulation

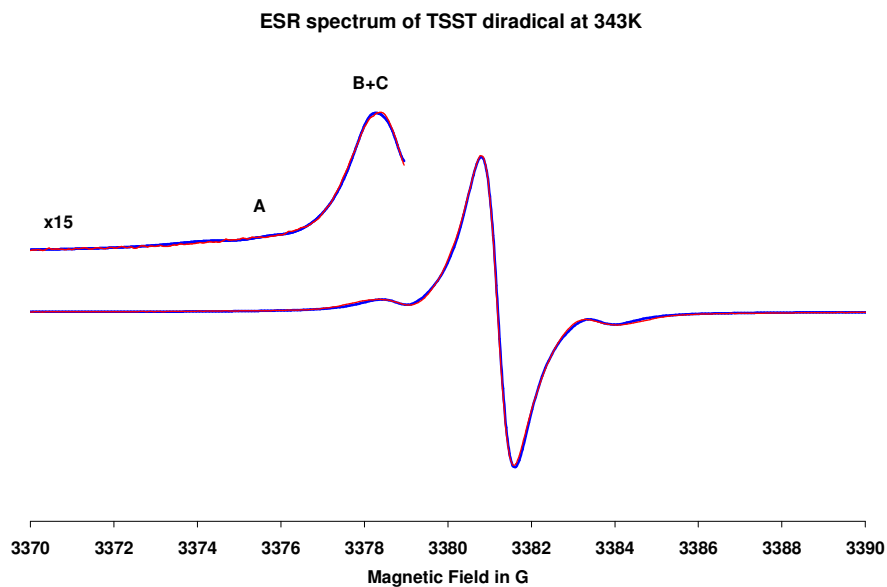


Figure S7. ESR spectrum of the diradical TSST at 343K in water. Red curve: experimental; blue curve: calculated. The ^{13}C satellites were interpreted as: A band: 1 carbon with hfsc 11.5 G; B band: 3 carbons with hfsc 5.5G; C band: 6 carbons with hfsc 4.7 G.

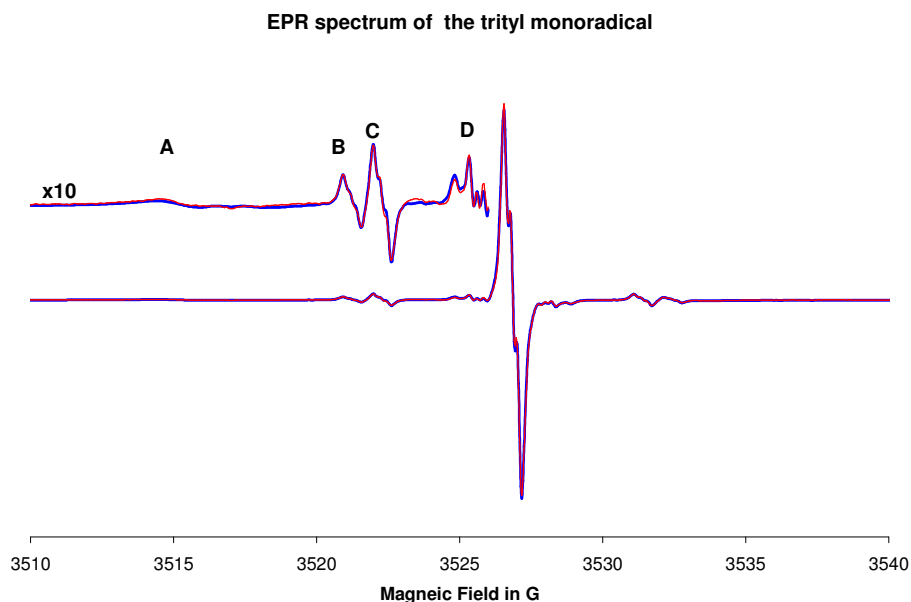


Figure S8. ESR spectrum of the trityl monoradical. Red curve: experimental, blue curve: calculated. The satellites are reconstructed as ^{13}C patterns. Band A: 1 carbon with the hfsc of 23.5 G, band B: 2 carbons with the hfsc of 11.26 G plus 1 carbon with the hfsc of 11.07 G, band C: 4 carbons with the hfsc of 9.16 G plus 2 carbons with the hfsc of 9.00 G,

band D: 1 carbon with the hfsc of 3.57 G, 2 carbons with the hfsc of 3.38 G, 4 carbons with the hfsc of 2.41 G, 2 carbons with the hfsc of 2.30 G.

Table S1. ZFS parameters and population of conformers for TSST in EG-water mixture

Conformer Temperature/K	A D in G	A E in G	A Population%	B D in G	B E in G	B Population%
223	12.76	2.24	81.4	6.22	0.80	18.6
233	12.34	2.19	80.9	5.86	0.74	19.1
243	11.47	2.06	80.6	5.40	0.71	19.4
263	9.94	1.77	54.8	3.35	0.33	45.2
283	8.23	1.06	42.9	2.46	0.35	57.1

Table S2. The g-, hyperfine- and zero-field tensors of TSSN in EG-water mixture at 153 K

	x	y	z
A_N in G	4.4	0	42.0
D in G*	-1.9	-2.7	4.6

*The zero-field parameters can be also given as D=6.9G and E=0.8G

VI. Reaction of TSSN with GSH detected by UV-Vis spectroscopy

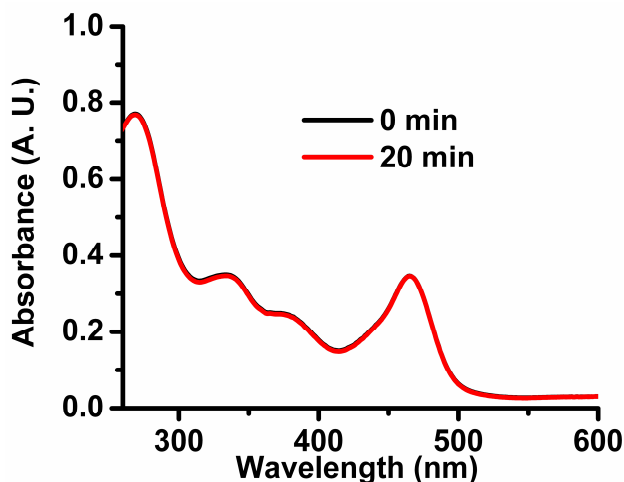


Figure S9. UV-Vis spectra of the reaction solution containing TSSN (20 μ M) and GSH (3 mM). The spectra were recorded at 0 and 20 min after GSH was added to the TSSN solution in PB (pH 7.4, 20 mM).

VII. Kinetic studies of TSSN and TSST with thiol compounds detected by EPR spectroscopy

Various concentrations of thiols were added to the solution of the biradical ($50 \mu\text{M}$) in PB (50 mM , $\text{pH } 7.4$). Incremental EPR spectra were recorded 60 s after mixing and this point was considered to be $t = 0$ in Figure S10-12. Since the thiol concentration used was in greater excess than the concentration of the biradical ($50 \mu\text{M}$), the reaction kinetics of the biradical with the thiol compound is a pseudo first-order reaction.

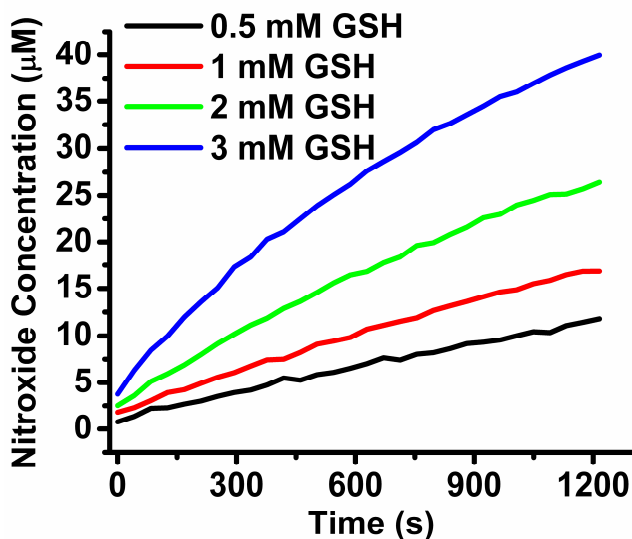


Figure S10. Formation kinetics of the nitroxide monoradical in the presence of TSSN ($50 \mu\text{M}$) and various concentrations of GSH.

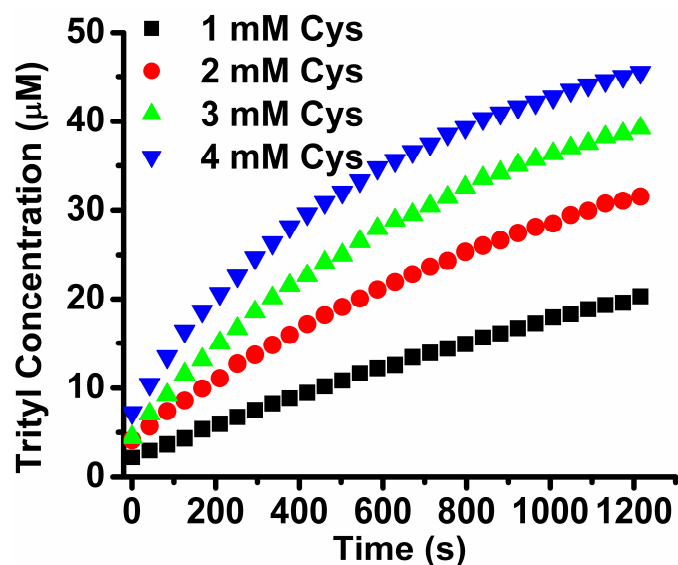


Figure S11. Formation kinetics of the trityl monoradical in the presence of TSSN (50 μM) and various concentrations of cysteine.

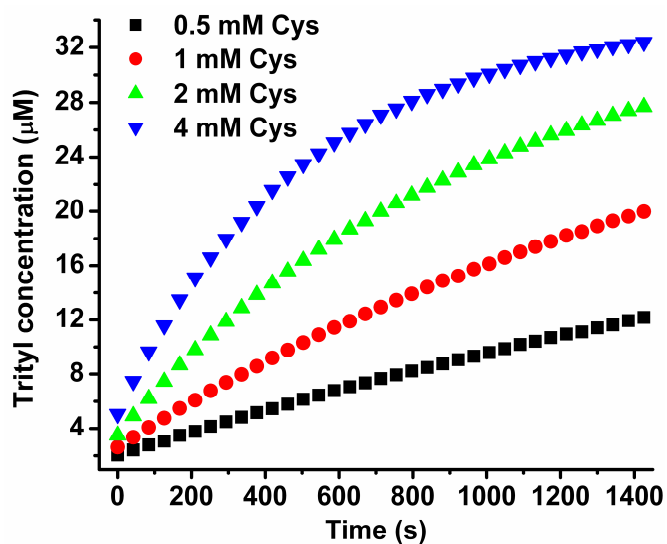


Figure S12. Formation kinetics of the trityl monoradical in the presence of TSST (20 μM) and various concentrations of cysteine.

VIII. Reaction of TSSN with ascorbate

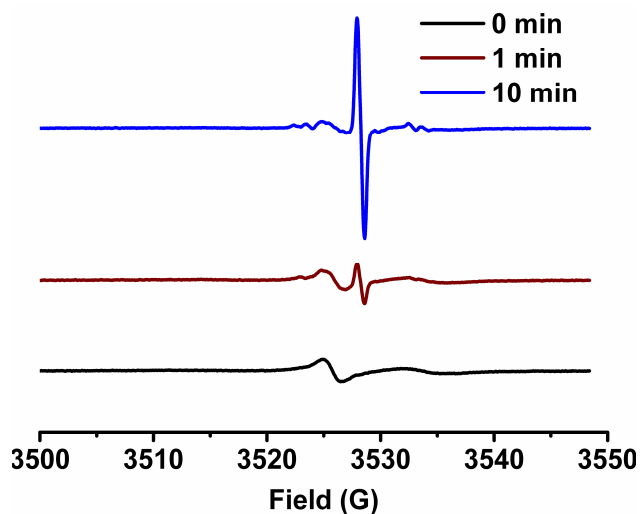


Figure S13. EPR spectra obtained by reaction of TSSN (50 μM) with ascorbate (2 mM) in PB (50 mM, pH 7.4).

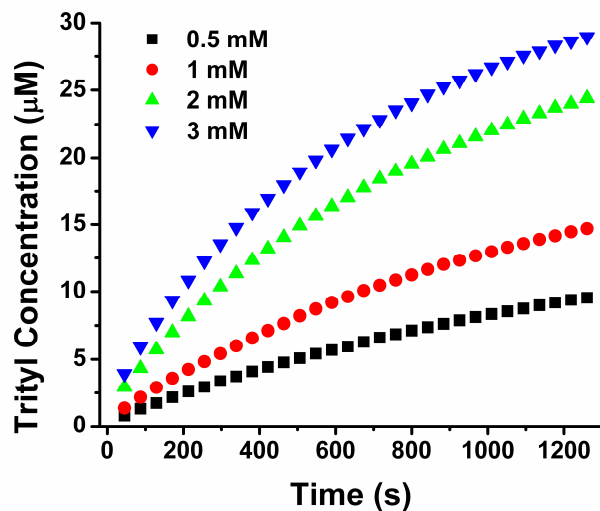


Figure S14. Formation kinetics of the trityl monoradical in the presence of TSSN (50 μM) and various concentrations of ascorbate in PB (50 mM, pH 7.4).

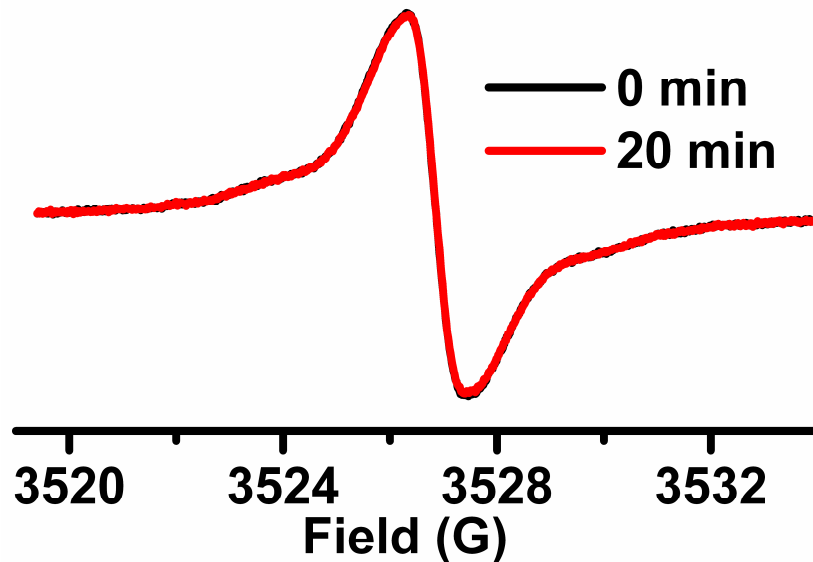


Figure S15. EPR spectra obtained by reaction of TSST (50 μM) with ascorbate (2 mM) in PB (50 mM, pH 7.4).

IX. Plot of UV-vis absorbance versus GSH concentration

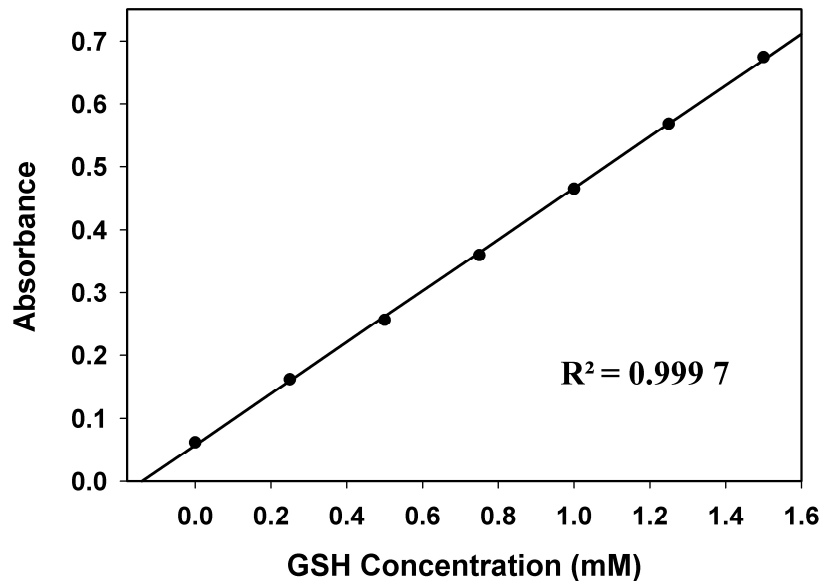


Figure S16. Plot of UV-vis absorbance versus GSH concentration. To a 96-well plate, the Ellman's reagent was added to various concentrations of GSH in PB (10 mM, pH 7.4) containing EDTA (200 μM).

X. Spectroscopic characterization

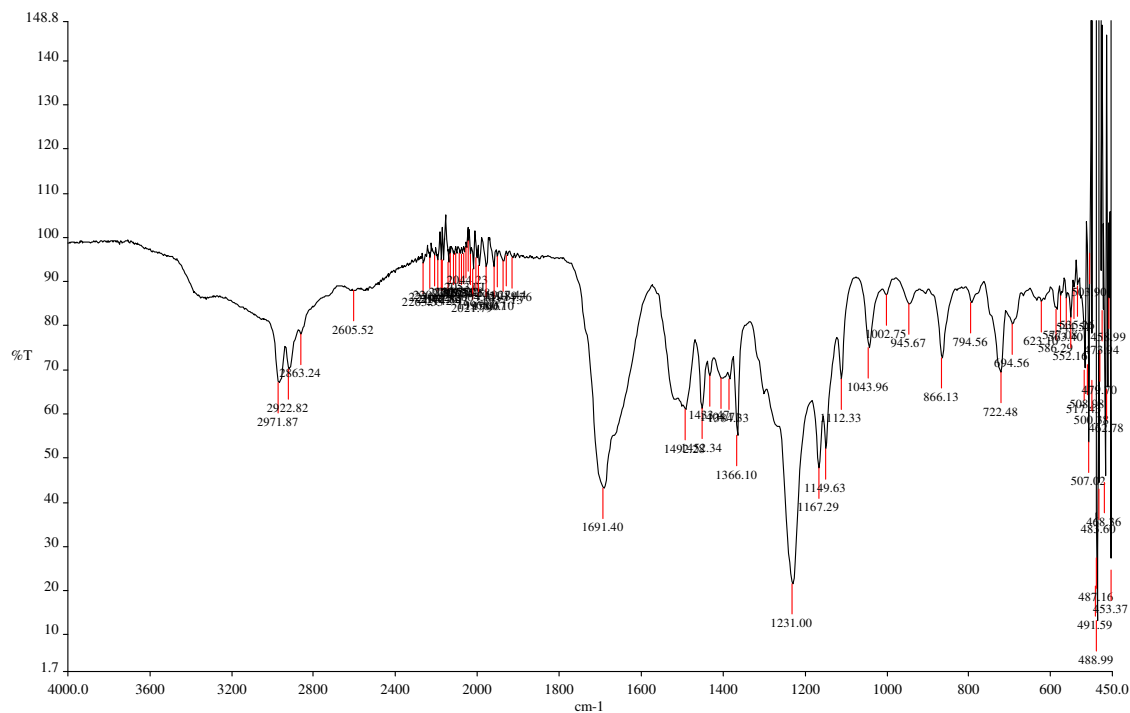


Figure S17. IR spectrum of TSS-Boc

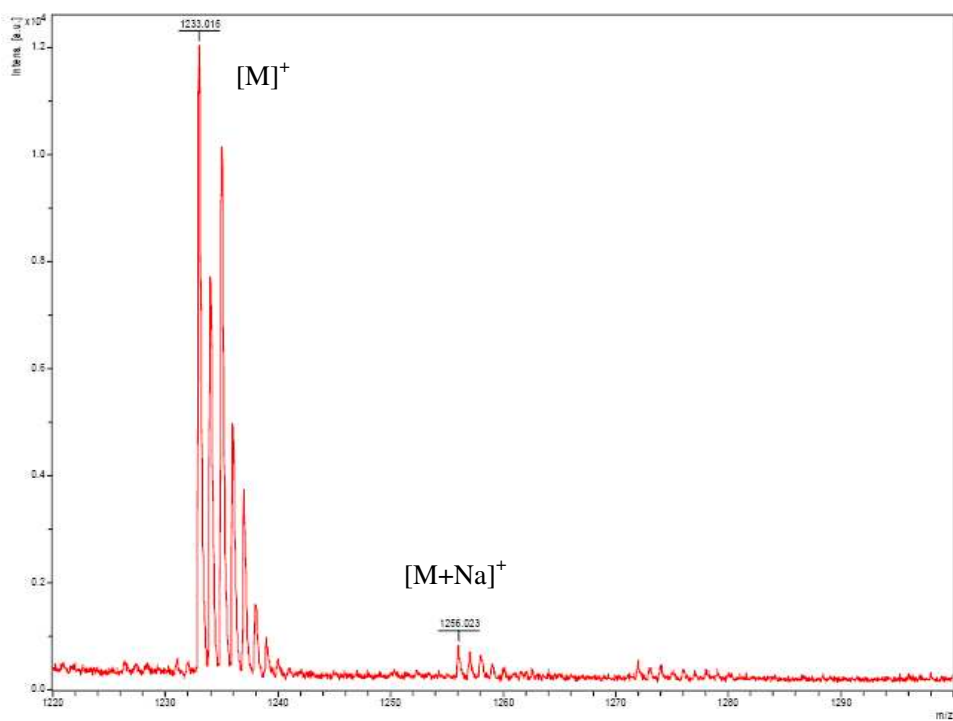


Figure S18. High Resolution Mass Spectrum of TSS-Boc

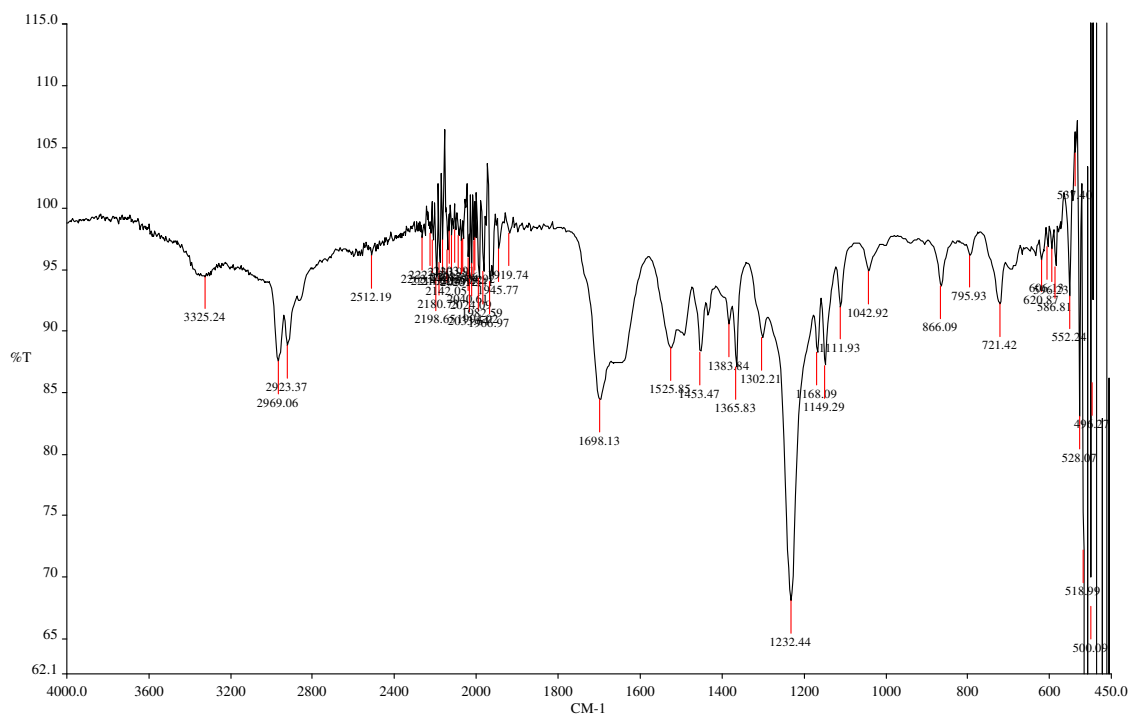


Figure S19. IR spectrum of TSSN

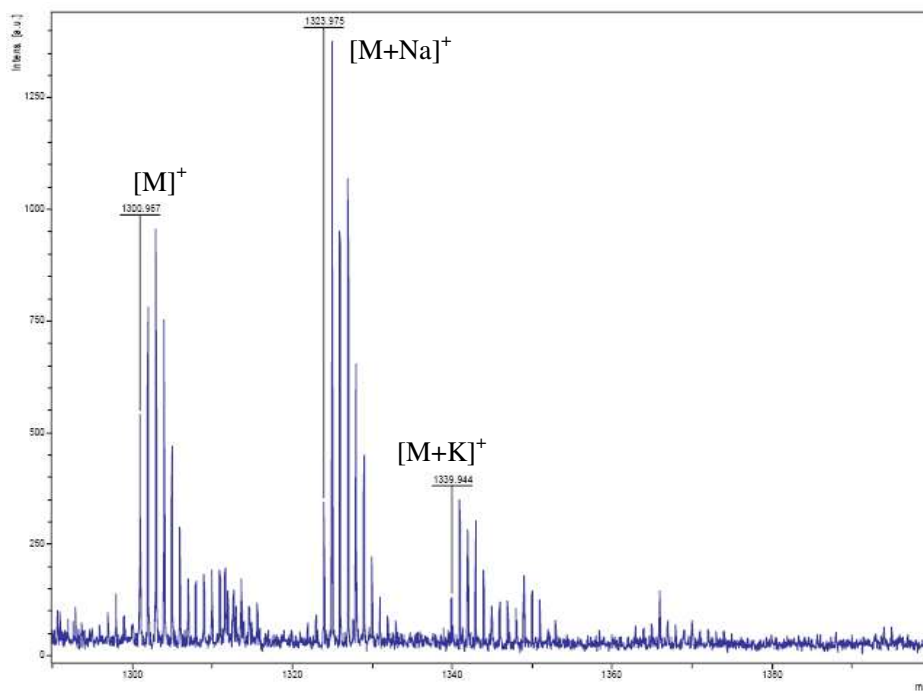


Figure S20. High Resolution Mass Spectrum of TSSN

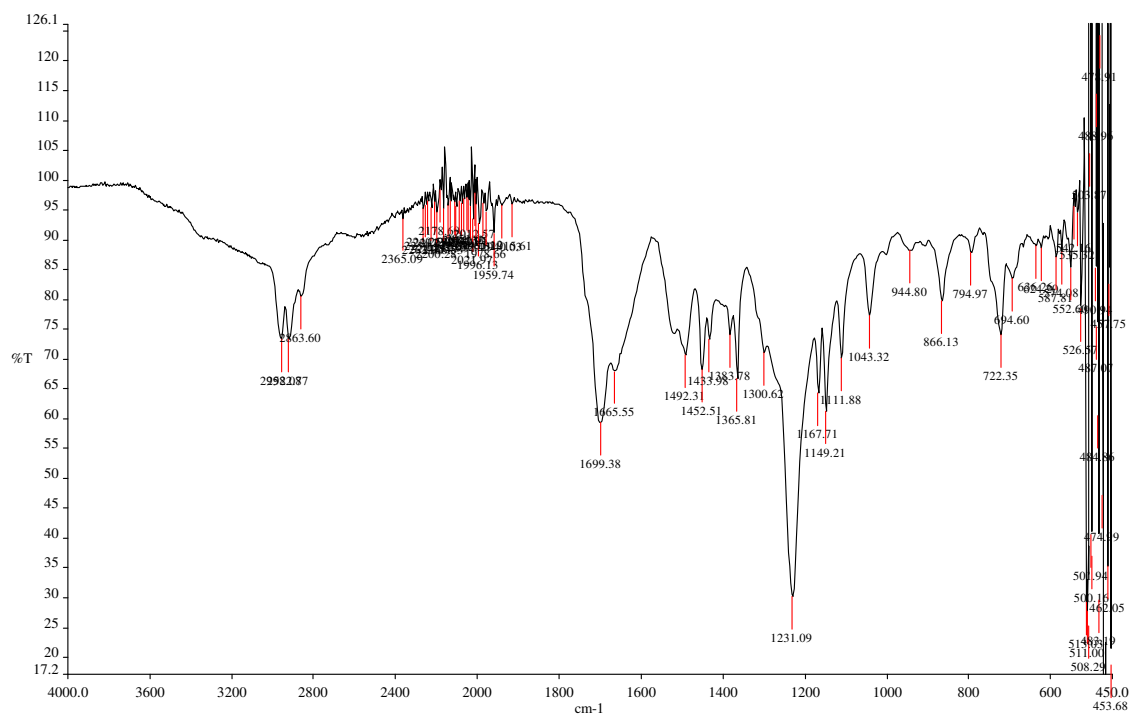


Figure S21. IR spectrum of TSST

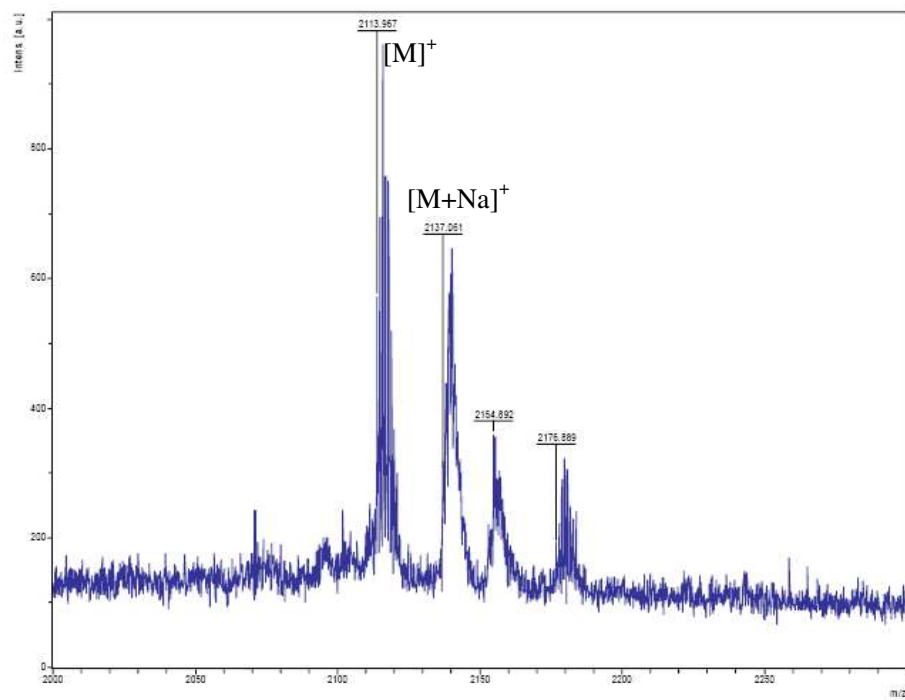


Figure S22. High Resolution Mass Spectrum of TSST